Recent Advances in High-Frequency Electron Spin Resonance Detection Using a Microcantilever

Hitoshi Ohta · Eiji Ohmichi

Abstract Our recent developments in highly sensitive high-frequency electron spin resonance (ESR) using a microcantilever are reviewed. ESR signals of a Co Tutton salt microcrystal (<1 μg) have been detected at low temperature at frequencies up to 315 GHz under a static magnetic field using a microcantilever and a modulation technique. The achieved sensitivity is about 10^9 spins/G at 4.5 K. Moreover, we have shown that similar ESR detection using a microcantilever is possible up to 130 GHz under a pulsed magnetic field without using a modulation technique. The achieved sensitivity is about 10^{11} spins/G at 1.7 K. These results suggest that the ESR detection using a microcantilever is promising for applications to high-resolution and high-sensitivity terahertz ESR.

1 Introduction

Commercial X-band electron spin resonance (ESR) is used in a wide range of research areas, such as biology, medicine, chemistry, physics, and so on, due to its high sensitivity of the order of 10^{10} spins/G and its easy access to the measurement system. Its high sensitivity is mainly supported by the use of a resonant cavity and of the modulation techniques and phase-sensitive detection [1]. However, there is a

H. Ohta (✉)
Molecular Photoscience Research Center, Kobe University,
1-1 Rokkodai-cho, Nada, Kobe 657-8501, Japan
e-mail: hohta@kobe-u.ac.jp

H. Ohta · E. Ohmichi
Graduate School of Science, Kobe University, 1-1 Rokkodai-cho,
Nada, Kobe 657-8501, Japan

H. Ohta
Headquarters for Innovative Cooperation and Development,
Kobe University, 1-1 Rokkodai-cho, Nada, Kobe 657-8501, Japan

strong demand to extend the ESR frequency to the higher frequency region because the high-frequency ESR has many advantages, such as the high spectral resolution, the ESR detection beyond the zero-field splitting, and the observation of a broad ESR line, etc. [2–4]. Therefore, there are many examples of high-frequency ESR results to date [5–12]. In most cases these measurements used aforementioned techniques together with a static field in order to maintain the high sensitivity; for instance, the sensitivity achieved above 200 GHz is of the order of 10^9 spins/G [11, 12]. Although, however, the resonator maintains the high sensitivity, it fixes the frequency of the measurement system. On the other hand, multifrequency ESR up to the terahertz region is becoming a powerful means to study magnetic systems with strong interactions because these systems often show a very broad line width of the order of 1 T and a very large zero-field splitting of the order of terahertz [3, 4, 13–16]. As the resonant cavity is not useful for the multifrequency ESR, these measurements are performed by the transmission method using the oversized lightpipe [3, 4, 13–16]. Moreover, as the resonance field at 1 THz exceeds the magnetic field of 20 T, which is typically the maximum field of the superconducting magnet, the pulsed magnetic field is often used for the measurement [3, 4, 17–19]. The frequency-field region covered by our multifrequency ESR system in Kobe University can be found in Refs. [3, 4]. However, such multifrequency ESR using the transmission method shows relatively poor sensitivity of the order of 10^{15} spins/G compared to the other high-frequency ESR using a resonant cavity and a modulation technique.

In order to overcome such difficulty of the multifrequency ESR in the terahertz region, we are developing the highly sensitive high-frequency ESR method using a microcantilever [20–23]. In this review, the overall results of the ESR detection using a microcantilever and a possible application to the terahertz ESR will be discussed.

2 Principle of Measurement

Here we consider the typical case of $S = 1/2$. The energy levels of the electron spin, that is, the up spin ($S_z = 1/2$) and the down spin ($S_z = -1/2$), are degenerate under the zero magnetic field. When the external field is applied, two energy levels split by the energy of $g\mu_B B$, which is called the Zeeman splitting, where g, μ_B, and B are the g-factor, Bohr magneton, and the external magnetic field, respectively. The distribution ratio between the up and down spins obeys the Boltzman distribution determined by the Zeeman splitting and the temperature. ESR is the resonant absorption of the electromagnetic wave when the energy of the electromagnetic wave $h\nu$ and the Zeeman energy coincide. Therefore, the resonance condition of ESR is $h\nu = g\mu_B B$, and the ESR signal is detected by measuring the absorbed power of the electromagnetic wave in the conventional ESR. On the other hand, the ESR absorption accompanies the spin reversal process, and this means that the magnetization of the system also changes at ESR absorption. Therefore, the basic idea of our ESR detection using a cantilever is to detect the change of the magnetization of the system instead of detecting the change of the power absorption of the electromagnetic wave.

How can we detect such a change of the magnetization? Let us consider a paramagnetic system under a uniform magnetic field $\mathbf{B}$. The system is magnetized because the magnetization is proportional to the distribution difference between the down spin and the up spin, and the magnetic torque defined by $\boldsymbol{\tau} = \mathbf{M} \times \mathbf{B}$ acts on the system, where $\mathbf{M}$ is the magnetization. It is shown previously by Ohmichi et al. [24] that the highly sensitive magnetic torque measurement can be achieved even under the pulsed magnetic field by fixing a magnetic sample on a microcantilever. Therefore, our idea of the ESR detection is the observation of the magnetic torque by using a microcantilever [20, 21]. The magnetic anisotropy is required for the torque measurement because $\mathbf{M}$ is parallel to $\mathbf{B}$ for a magnetically isotropic system. As, however, the $\mathbf{g}$-tensor anisotropy often exists in paramagnetic systems, the ESR detection is possible by using a microcantilever.

Our ESR detection using a microcantilever has the following advantages: as the size of the cantilever is of the order of 100 μm, the ESR detection in a microcrystal of the order of 1 μg is possible. This enables the highly sensitive detection of ESR comparable to the method using a resonant cavity or a Fabry–Perot resonator. Moreover, the cavitiless and wide band detection of cantilever ESR is very suitable for the multifrequency ESR because the operating frequency can be changed easily by replacing the electromagnetic sources for the cavitiless system, and the torque measurement of ESR has no limitation to the operating frequency, in principle. Therefore, the cantilever ESR system becomes a very simple system, that is, the microcantilever with a sample is placed at the center of the magnet, and the electromagnetic wave is guided to the sample by an oversized lightpipe, in a manner similar to the transmission-type ESR. The microcantilever serves as a highly sensitive detector and its relatively high eigenfrequency ($f \sim 10$–100 kHz) enables the detection even under the strong pulsed magnetic field [24]. All these features suggest that the ESR detection using a microcantilever is promising for highly sensitive ESR applications in the terahertz region.

Finally, we would like to point out that our method is in contrast to the magnetic resonance force microscopy (MRFM) [25, 26], which is also based on the mechanical detection using a cantilever. In MRFM, the force from the sample surface, which is represented by $\mathbf{F} = \text{grad}(\mathbf{H} \cdot \mathbf{M})$, is detected by a magnetic tip on a cantilever, which is producing the field gradient. ESR is also detected from the change of the magnetization $\mathbf{M}$, but the way of detecting the change is different from our torque measurement. Due to the existence of the field gradient, MRFM has the high spatial resolution of the order of 1 nm, while the spectral resolution is limited by the low operating frequency of about 1 GHz because the high magnetic field will saturate the magnetization of the magnetic tip, and its application to the high-frequency ESR in the terahertz region will be difficult. In this sense, the possible application in the terahertz region is the most characteristic feature of our microcantilever ESR system.

3 Experimental Setups

The cantilever used in our study was a piezoresistive microcantilever, which was commercially available for use with atomic force microscopy [27] (Fig. 1).
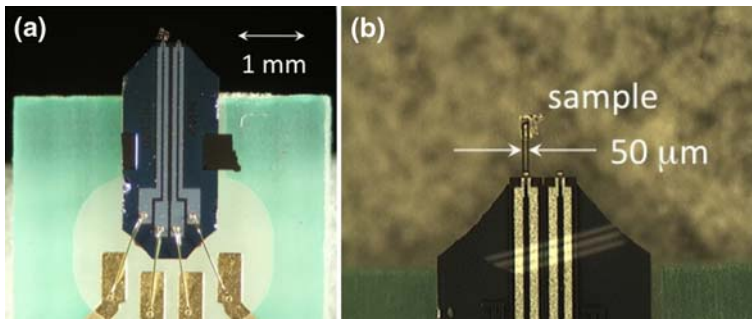
Fig. 1 **a** Optical microscope image of the whole cantilever. The cantilevers are fabricated at the *upper end*, and the base of the cantilever is fixed to a plastic plate and is wire-bonded for electrical connections. **b** Magnified view of the cantilever. The measurement lever with the sample (*left*) and the compensation lever (*right*) can be seen

Different types of cantilever were used for the static and the pulsed magnetic fields as shown in Table 1. The cantilever with a lower eigenfrequency was used for the static field in order to match the modulation frequency of the electromagnetic wave source, while the cantilever with a higher eigenfrequency was used for the pulsed field in order to achieve a fast mechanical response during the pulse duration of the field, which was typically about 10 ms. A piezoresistive path was fabricated by the ion plantation with boron at the cantilever legs, and a magnetic torque acting on the cantilever beam was detected through the change of the piezoresistance. The piezoresistance monotonically decreased upon cooling and was typically 550–600 Ω at 4.2 K. A small change in the piezoresistance was measured using a Wheatstone bridge circuit, and a compensation lever (see Fig. 1), which is fabricated on the same substrate, was used to eliminate the thermal drift and the magnetoresistance effect.

The sample used in our study was a single crystal of Co Tutton salt, $Co(NH_4)_2(SO_4)_2 \cdot 6H_2O$ [28–30], which is a paramagnet with anisotropic *g*-values arising from the Ising nature of the Co^{2+} ion. A single crystal was mounted onto the cantilever beam with a small amount of epoxy adhesive using a miniature *XYZ* stage under a microscope. The sample size was typically 50–100 µm, and the sample mass was about 0.5–5 µg, which was roughly estimated from the eigenfrequency shift.

For the measurement under the static magnetic field, 4 and 7 T superconducting magnets were used. As shown in Fig. 2a, an electromagnetic wave was introduced through a lightpipe from the top of the cryostat and was focused to the sample fixed on the cantilever using a conical brass horn. Gunn oscillators and multipliers in the

Table 1 Cantilevers used in our study

Dimension (µm^3)	Spring constant (N/m)	Eigenfrequency (kHz)	Magnetic field
400 × 50 × 5	2–3	35–40	Static
120 × 50 × 5	30–40	250–300	Pulse

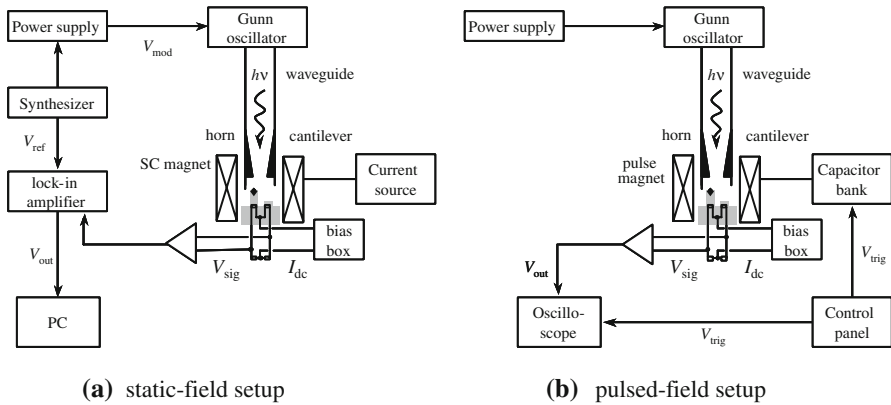**(a)** static-field setup   **(b)** pulsed-field setup

Fig. 2 **a** Schematic block diagram of the ESR detection system under the static magnetic field [20].
b Schematic block diagram of the ESR detection system under the pulsed magnetic field [21]

frequency range of 80–315 GHz were used as light sources. The measurement
scheme is summarized in Fig. 2a. The output power of the light source was
externally modulated at the modulation frequency f_{mod} using a synthesizer.
Therefore, the output voltage of the bridge circuit was modulated at the ESR
absorption. The modulated signal was amplified and sent to a lock-in amplifier
whose reference signal was externally fed by the synthesizer. By adjusting f_{mod} to
coincide with the eigenfrequency of the loaded cantilever, the output signal can be
resonantly enhanced (see Ref. [21] for details).

For the measurement under the pulsed magnetic field, the pulse magnets and the
capacitor banks, which were installed at Kobe University, were used [17]. The
measurement scheme is shown in Fig. 2b. Gunn oscillators in the frequency range
of 60–130 GHz were used as light sources. A lightpipe and a horn similar to the
case of the static magnetic field were used. However, no lock-in technique was
employed and the measurement was essentially the direct current (dc) method. The
output voltage from the bridge circuit was amplified and recorded with a data-
storage oscilloscope at the sampling rate of 1 megasample/s. A compensation coil
was used to cancel the voltage induced in the circuit by the pulsed magnetic field
(see Ref. [22] for details).

4 Results and Discussion

4.1 Under the Static Magnetic Field [21, 23]

Figure 3a shows typical ESR absorption lines obtained by dc and modulation methods
at 80 GHz and 4.5 K. The standard four-terminal method is used for the dc
measurement. The measurements are carried out in ^{4}He exchange gas condition. The
pressure is set to 200 Torr to suppress the spurious excitation of cantilever vibration
due to the light intensity modulation. Although broad ESR absorption lines are
observed at 1.26 T for both cases, the signal-to-noise ratio obtained by the modulation

method is much better than that obtained by the dc method. When the magnetic field is applied on the paramagnetic Co Tutton salt, the magnetization appears in proportion to the magnetic field. Therefore, the magnetic torque due to the ESR absorption is superposed on the larger background torque coming from the magnetization in the dc method, and this background signal is subtracted for clarity in Fig. 3a. On the other hand, as the output power of the electromagnetic wave is modulated in the modulation
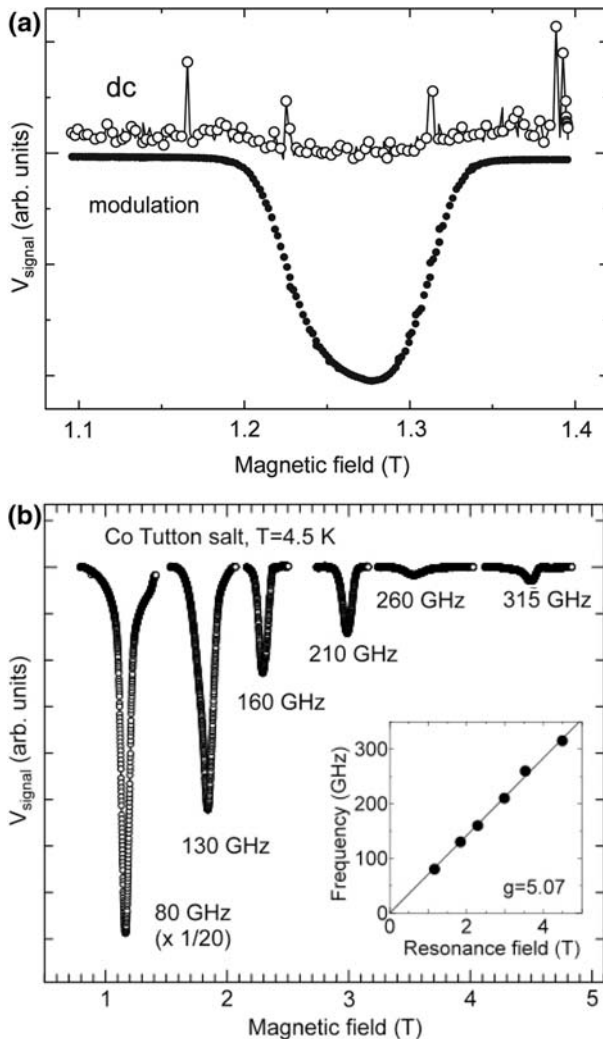

Fig. 3 a ESR absorption lines obtained by dc (*open circles*) and modulation (*solid circles*) methods in the ⁴He gas condition with the same bias current. **b** Typical ESR absorption lines observed at 4.5 K in the frequency region from 80 to 315 GHz. The modulation technique shown in Fig. 2a and the static magnetic field are used. The background signal was subtracted for clarity. The *inset* shows the frequency-field relation of the observed resonances. A linear fit, which is indicated by the *solid line*, gives the g-value of 5.07

method, the background torque from the magnetization can be eliminated effectively and only the torque change coming from the ESR absorption can be extracted. Moreover, the output signal coming from ESR in the modulation method is resonantly enhanced by adjusting the modulation frequency of the electromagnetic wave to coincide with the eigenfrequency of the loaded cantilever. In turn, the signal-to-noise ratio obtained by the modulation method can be greatly improved. In the optimal condition, which is the modulation frequency of about 9360 Hz in the ^{4}He gas condition, the signal-to-noise ratio of about 10^3 is achieved for the modulation method at 80 GHz and 4.5 K. The minimum detectable spin number is estimated to be about 10^{12} spins by taking into account the sample mass of about 0.9 μg. Considering the ESR line width of about 90 mT, the obtained sensitivity for the modulation method under the static magnetic field is about 10^9 spins/G. This sensitivity is two orders of magnitude better than that of the dc method under the pulsed magnetic field, which will be discussed in the next section. In the present setup, the sensitivity is limited by both mechanical and electrical noises because the thermal noise is found to be negligible compared to those under the low-temperature condition of 4.5 K. The mechanical noise may be reduced by suspending the cryostat to isolate the vibration from the floor, and there may be also some room to reduce the electrical noise. If noise sources other than thermal noise can be ignored, the sensitivity can approach much better value like 10^7 spins/G because the detectable magnetic torque is estimated to be on the order of 10^{-17} Nm (see Ref. [21] for details). We should point out that the sensitivity discussed here depends on the g-anisotropy and the spin relaxation time [1]. Therefore, the sensitivity may change from sample to sample.

Figure 3b shows the ESR absorption lines observed at different frequencies by the modulation technique using the superconducting magnet up to 7 T. The modulation frequency is set to the eigenfrequency of the loaded cantilever in order to enhance the ESR signals. The inset of Fig. 3b shows the frequency-filed relation of the observed signals. As the linear fit to the observed results crosses the origin, the obtained signals in Fig. 3b can be considered as the ESR signals from the paramagnet. Moreover, the g-value of 5.07 obtained from the inset of Fig. 3b is consistent with the reported g-values of Co Tutton salt [30]. The signal intensity depends strongly on the output power of the Gunn oscillators and the multipliers, which tends to decrease as the frequency increases. Although the output power is 80 mW for the Gunn oscillator at 80 GHz, it decreases to less than 5% of that of the fundamental Gunn oscillator for the multipliers above 160 GHz, and it is about 1 mW at 315 GHz. Nevertheless, we have succeeded in observing ESR at 315 GHz, which is the highest frequency achieved for the cantilever ESR to our knowledge. By using the higher frequency source, such as backward wave oscillators (250 GHz–1.2 THz) in Kobe University, and the 15 T superconducting magnet, which will be installed soon, the cantilever ESR at 1 THz using the modulation technique may be possible in near future.

4.2 Under the Pulsed Magnetic Field [20, 22]

Figure 4 shows the waveform of the pulsed magnetic field and the output signals from the bridge circuit, where ON and OFF in the figure denote the output voltages with and without an electromagnetic wave irradiation, respectively. The sample

with the mass of 0.8 μg and the 100 kJ capacitor bank are used. The magnetization from the paramagnetic Co Tutton salt under the magnetic field appears as a background magnetic torque even without the irradiation (OFF signal), while the ESR signal from the sample is superposed on a background magnetic torque (ON signal). Therefore, ESR signals clearly remain in both up and down sweeps of the magnetic field as shown by the ON–OFF curve in Fig. 4, which is the result of the subtraction of the OFF voltage from the ON voltage. By plotting the ON–OFF curve versus the magnetic field, the field dependence of the ESR signal as shown in Fig. 5a and the ESR resonance field can be obtained.

Multifrequency ESR can be performed easily by replacing only the Gunn oscillator in Fig. 2b. ESR signals have been obtained successfully up to 130 GHz in the pulsed magnetic field as shown in Fig. 5a. As the output power of the Gunn oscillator decreases with increasing frequency, this seems to limit the ESR observation beyond 130 GHz under the present setup. Obtained mutifrequency ESR results are plotted in the frequency–field diagram as shown in Fig. 5b. As the linear fit to the results crosses the origin, the obtained signals in Fig. 5a can be considered as the ESR signals from the paramagnet. Moreover, the g-value of 3.71 obtained from Fig. 5b is consistent with the reported g-values of Co Tutton salt, which range between 3 and 6 due to the strong anisotropy of Co^{2+} ions in the Co Tutton salt [30]. Obtained g-value is different from that obtained in the case of the static magnetic field because the cantilever and the sample used in the measurements are different.

In order to compare the sensitivity of our cantilever ESR method with that of the transmission method, ESR measurement of the Co Tutton salt single crystal using our transmission method has been also performed. The results obtained at 80 GHz and 1.7 K are shown in Fig. 6. The sample mass for the transmission measurement is 4 mg, which is about 5×10^3 times heavier than the sample used in the cantilever
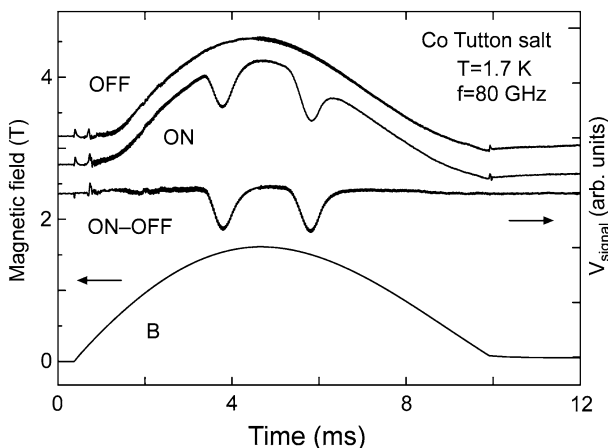

Fig. 4 Waveform of the pulsed magnetic field and the output voltages from the cantilever bridge circuit are shown as a function of time. ON and OFF in the figure denote the output voltages with and without an electromagnetic wave irradiation, respectively. The subtraction of the OFF voltage from the ON voltage is denoted as ON–OFF, and clear ESR signals are obtained. The operating frequency and the sample temperature are 80 GHz and 1.7 K, respectively
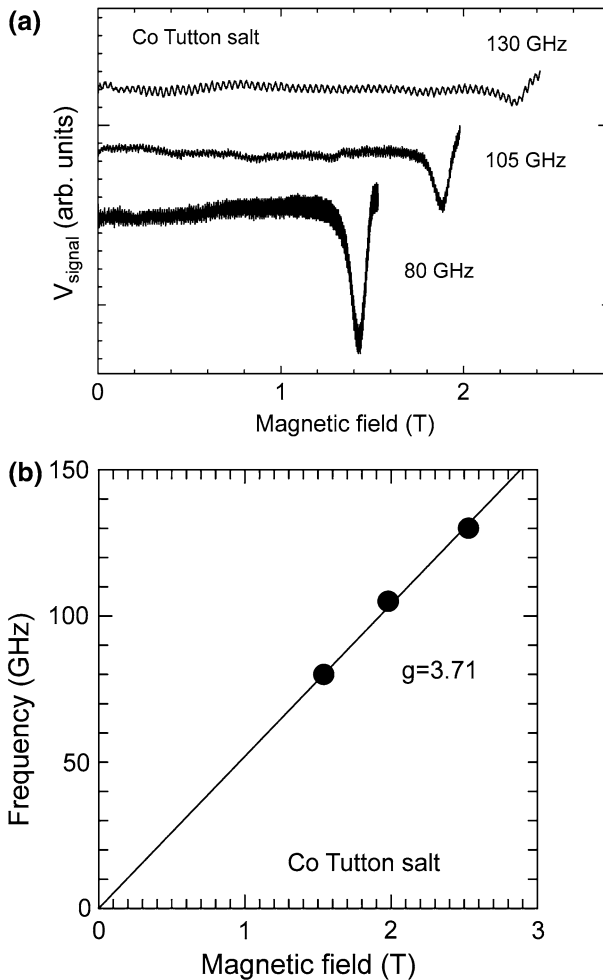
Fig. 5 **a** Output signal versus magnetic field obtained at 1.7 K. The background signals are subtracted for clarity. **b** Frequency-field relation obtained at 1.7 K. The result clearly shows a paramagnetic behavior with $g = 3.71$

ESR. Nevertheless, it is clear from Fig. 6 that the signal-to noise ratio is even better for the cantilever ESR. The minimum detectable number of spins for the cantilever ESR is estimated to be about 10^{14} spins from a signal-to-noise ratio of about 15 and a sample mass of about 0.8 μg. Therefore, the sensitivity of our cantilever ESR is estimated to be about 10^{11} spins/G by taking into account the ESR line width of about 90 mT. On the other hand, the sensitivity of our transmission method is estimated to be about 10^{15} spins/G from Fig. 6. Therefore, we can say that the sensitivity of our cantilever ESR is about 10^4 times better than that of our transmission method.

Here, we would like to discuss the origin of the dominant noise in our cantilever ESR using the pulsed magnetic field. In Fig. 5a the oscillatory noise can be seen in
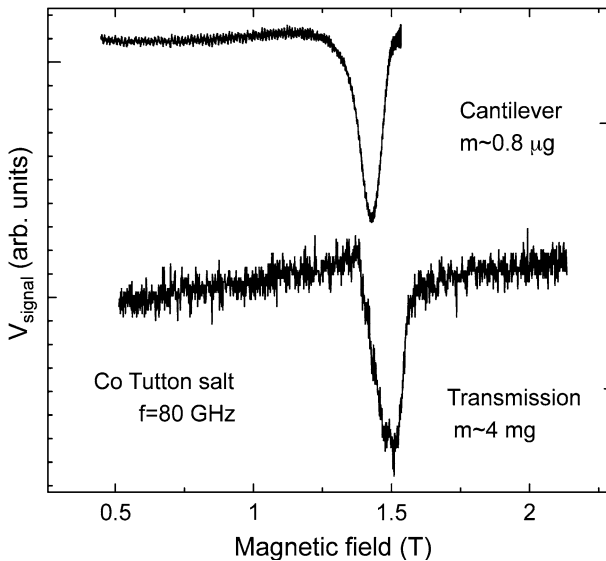
Fig. 6 ESR signals obtained by the cantilever method (*upper curve*) and the transmission method (*lower curve*) at 80 GHz and 1.7 K. The *vertical scale* is normalized and offset for clarity

the ESR signal registered at 130 GHz. This oscillation is periodic in time and the frequency is common for all cases including the results for 80 and 105 GHz. The oscillation frequency of the noise is estimated to be 30.5 kHz. As this value coincides with the eigenfrequency of the sample-loaded cantilever, it suggests that the oscillatory noise is coming from the mechanical vibration of the cantilever itself, which was negligible in the cantilever ESR measurement under the static field. An electromagnetic force between the electrodes of a pulsed magnet will induce the vibration at the capacitor discharge, and this may excite the mechanical vibration of the cantilever itself. Therefore, the cantilever ESR measurement using a long-pulse magnet or a crowbar circuit, which extends the down-field sweep time to 100–200 ms, will reduce the mechanical vibration noise because a decay time of the vibration is typically 10–20 ms. Then the cantilever ESR detection using the pulsed magnetic field may be extended beyond 130 GHz and into the terahertz region.

5 Summary

Our developments in highly sensitive high-frequency ESR using a microcantilever are reviewed. Two approaches, which use the static magnetic field and the pulsed magnetic field, are shown. In the case of the static field, the modulation technique is employed and the sensitivity of about 10^9 spins/G is achieved at 4.5 K. This enables the high-frequency ESR detection of less than 1 μg Co Tutton salt up to 315 GHz, which is the highest frequency achieved for the cantilever ESR to our knowledge. On the other hand, it is also shown that the cantilever ESR detection by the dc method under the pulsed magnetic field is possible at 1.7 K. The achieved frequency

and sensitivity are 130 GHz and 10^{11} spins/G, respectively. Our results suggest that the cantilever ESR is promising for the future applications to the high-resolution and high-sensitivity terahertz ESR.

References

1. C.P. Poole Jr., *Electron Spin Resonance*, 2nd edn. (Dover, New York, 1996)
2. S.S. Eaton, G.R. Eaton, in *Handbook of Electron Spin Resonance*, vol. 2, ed. by C.P. Poole Jr. (Springer, New York, 1999), p. 345
3. H. Ohta, S. Okubo, K. Kawakami, D. Fukuoka, Y. Inagaki, T. Kunimoto, Z. Hiroi, J. Phys. Soc. Jpn. **72** (Suppl. B), 26–35 (2003)
4. M. Motokawa, H. Ohta, N. Makita, Int. J. Infrared MMW **12**, 149 (1991)
5. E. Reijerse, P.P. Schmidt, G. Klihm, W. Lubitz, Appl. Magn. Reson. **31**, 609 (2007)
6. K. Möbius, Biol. Magn. Reson. **13**, 253 (1993)
7. W.B. Lynch, K.A. Earle, J.H. Freed, Rev. Sci. Instrum. **59**, 1345 (1988)
8. P.A.S. Cruickshank, D.R. Bolton, D.A. Robertson, R.J. Wylde, G.M. Smith, Joint 32nd International Conference on Infrared and Millimeter Waves and 15th International Conference on Terahertz Electronics, vols. 1&2 (2007), 79–81
9. Y. Iwasaki, K. Katano, Y. Ohba, S. Karawasa, N. Koga, S. Yamauchi, Appl. Magn. Reson. **23**, 377–391 (2003)
10. K. Maeda, T. Hara, K. Furukawa, T. Nakamura, Bull. Chem. Soc. Jpn. **81**, 84–90 (2008)
11. H. Blok, J.A.J.M. Disselhorst, S.B. Orlinskii, J. Schmidt, J. Magn. Reson. **166**, 92 (2004)
12. J. van Tol, L.-C. Brunel, R.J. Wylde, Rev. Sci. Instrum. **76**, 074101 (2005)
13. H. Ohta, M. Sumikawa, M. Motokawa, H. Kikuchi, H. Nagasawa, J. Phys. Soc. Jpn. **65**, 848–852 (1996)
14. S. Kimura, K. Kindo, H. Tanaka, Physica B **346–347**, 15–18 (2004)
15. H. Nojiri, H. Kageyama, K. Onizuka, Y. Ueda, M. Motokawa, J. Phys. Soc. Jpn. **68**, 2906 (1999)
16. S.A. Zvyagin, A.K. Kolezhuk, J. Krzystek, R. Feyerherm, Phys. Rev. Lett. **93**, 027201/1-4 (2004)
17. H. Ohta, M. Tomoo, S. Okubo, T. Sakurai, M. Fujisawa, T. Tomita, M. Kimata, T. Yamamoto, M. Kawauchi, K. Kindo, J. Phys. Conf. Ser. **51**, 611–614 (2006)
18. S. Kimura, K. Kindo, Y. Narumi, M. Hagiwara, H. Kikuchi, Y. Ajiro, J. Phys. Soc. Jpn. **72** (Suppl. B), 99–108 (2003)
19. H. Nojiri, M. Motokawa, K. Okuda, H. Kageyama, Y. Ueda, H. Tanaka, J. Phys. Soc. Jpn. **72** (Suppl. B), 109–116 (2003)
20. H. Ohta, M. Kimata, S. Okubo, E. Ohmichi, T. Osada, AIP Conf. Proc. **850**, 1643–1644 (2006)
21. E. Ohmichi, N. Mizuno, M. Kimata, H. Ohta, Rev. Sci. Instrum. **79**, 103903/1-5 (2008)
22. E. Ohmichi, N. Mizuno, M. Kimata, H. Ohta, T. Osada, Rev. Sci. Instrum. **80**, 013904/1-5 (2009)
23. E. Ohmichi, N. Mizuno, M. Kimata, H. Ohta, J. Phys. Conf. Ser. **150**, 042150/1-4 (2009)
24. E. Ohmichi, T. Osada, Rev. Sci. Instrum. **73**, 3022–3026 (2002)
25. J.A. Sidles, Appl. Phys. Lett. **58**, 2854 (1991)
26. D. Rugar, R. Budakian, H.J. Mamin, B.W. Chui, Nature (London) **430**, 329 (2004)
27. Seiko Instruments Inc., 1-8 Nakase, Mihama-ku, Chiba 261-8507, Japan
28. W. Hofmann, Z. Krystallogr. **78**, 279 (1931)
29. T.N. Margulis, D.H. Templeton, Z. Krystallogr. **117**, 344 (1962)
30. B. Bleaney, D.J.E. Ingram, Proc. R. Soc. Lond. Ser. A **208**, 143 (1951)